Journal of Polymer Research (2021) 28:38
https://doi.org/10.1007/s10965-021-02411-6

ORIGINAL PAPER

X-ray diffraction and Raman study of pressure-assisted photopolymerization in the ferrocene-doped C_{60} crystals

K. P. Meletov[1] · A. V. Kuzmin[1] · S. S. Khasanov[1] · D. V. Konarev[2]

Received: 8 October 2020 / Accepted: 7 January 2021

Abstract

The pressure-assisted photopolymerization in the fullerene complex with ferrocene $C_{60}\cdot\{Fe(C_5H_5)_2\}_2$ was studied for the first time by simultaneous *in-situ* Raman and X-ray diffraction (XRD) techniques at pressures up to 8 GPa. The irreversible splitting of the $A_g(2)$ mode in the Raman spectra, resembling pristine fullerene polymerization, was observed at 4.6 GPa. The structural analysis does not show the formation of covalent bonds between adjacent fullerene molecules at a pressure up to 5 GPa. The unit cell volume and interfullerene distances are smooth and monotonous functions of pressure, and the shortest interfullerene distance 9.4 Å at 5 GPa significantly exceeds 9.06 Å typical of fullerene polymers. The changes in the Raman spectra at 4.6 GPa grow with the laser power and exposure time, showing typical photopolymerization phenomena. The distance between ferrocene and fullerene molecules decreases linearly with pressure changing the slope at 2 GPa due to intermolecular interaction crossover. The length of a ferrocene molecule in the complex increases with pressure in contrast to its decrease in a pristine ferrocene crystal. This behavior is associated with a change in the charge state of an iron atom and indicates a charge transfer from ferrocene to fullerene molecules.

Keywords Polymerization · Fullerene complexes · High pressure · Raman spectroscopy · X-ray analysis

Introduction

The fullerene molecular complexes are interesting for studies at high pressure because of their layered structure in which close–packed molecules in fullerene layers alternate with molecular donor layers. The reduction of intermolecular distances at high pressure increases the overlap of the highest occupied molecular orbital (HOMO) of the molecular donor and the lowest unoccupied molecular orbital (LUMO) of the fullerene acceptor that can stimulate a charge transfer. At the same time, a decrease in the intermolecular distances raises the possibility of covalent bonding between molecules in fullerene layers. Generally, the studies of fullerene complexes at high pressure are aimed at finding the pressure-induced charge transfer from a molecular donor to an acceptor C_{60} molecule and/or fullerene polymerization in the C_{60} layers of complexes. The behavior of various fullerene complexes at high pressure was studied in a number of publications, and the pressure-induced charge transfer, as well as the pressure-induced polymerization in fullerene layers have been reported many times [1–6].

The ability of pristine C_{60} to form intercage covalent bonds is due to the existence of 30 unsaturated double C = C bonds in the fullerene molecule. The polymerization of fullerene was observed for the first time in thin films or surfaces of bulk samples under illumination by visible light, owing to the small penetration depth of the light; the photopolymerized material is rather disordered and contains various C_{60} oligomers [7–9]. On the other hand, the treatment of C_{60} fullerene under various conditions of high pressure and high temperature (HPHT) results in formation of bulk ordered crystalline polymers. XRD studies of carefully prepared HPHT fullerene polymers have identified their crystal structures as one-dimensional orthorhombic (1D-O), two-dimensional tetragonal (2D-T) and two-dimensional orthorhombic (2D-O) [10, 11]. The infrared absorption and Raman spectra studies of fullerene polymers show the splitting and softening of the intramolecular phonon modes of C_{60} due to the formation

---

✉ K. P. Meletov
mele@issp.ac.ru

[1] Institute of Solid State Physics RAS, Chernogolovka, Moscow region 142432, Russia

[2] Institute of Problems of Chemical Physics RAS, Chernogolovka, Moscow region 142432, Russia

of intermolecular covalent bonds via [2 + 2] cyclo-addition mechanism and the concomitant symmetry and molecular stiffness reduction [12, 13]. Spectroscopic examination of the C_{60} polymers is based on the behavior of the $A_g(2)$ pentagon-pinch mode of the C_{60} cage, corresponding to the in-phase stretching vibration that involves tangential displacements of carbon atoms with a contraction of the pentagonal rings and an expansion of the hexagonal rings. In the C_{60} polymers, the $A_g(2)$ mode downshifts due to the decrease of the mean intramolecular bond strength. The softening depends on the number of the sp^3-like coordinated carbon atoms per fullerene molecular cage, associated with intermolecular covalent bond formation. The $A_g(2)$ mode of the *fcc* C_{60} monomer appearing at 1468 cm^{-1} downshifts to 1458 cm^{-1} in the 1D-O polymer (4 sp^3-like coordinated carbon atoms). In the 2D-T polymer (8 sp^3-like coordinated carbon atoms), the peak further downshifts to 1446 cm^{-1}, while in the case of the 2D-R phase (12 sp^3-like coordinated carbon atoms) the $A_g(2)$ mode exhibits the largest softening and is observed at 1408 cm^{-1} [10–12, 14, 15].

The pressure behavior of fullerene molecular complexes is studied usually by *in-situ* Raman spectroscopy at high pressure. The pressure-induced formation of covalent bonds between molecules in fullerene layers is always concluded from typical changes in Raman spectra related with $A_g(2)$ mode softening [1, 2, 5, 6]. However, these changes may be due to photo-induced polymerization in laser spot of ~ 2 mkm in daiameter and depth caused by laser irradiation during Raman measurements as in the case of thin C_{60} films under intense visible light or laser irradiation [7]. For example, the Raman spectra of the $\{Cd(dedtc)_2\}_2 \bullet C_{60}$ fullerene molecular complex, which are insensitive to durable laser irradiation at ambient conditions, show laser intensity and irradiation time dependent changes at elevated pressure resulting in softening of the $A_g(2)$ mode [4]. The photopolymerisation in the laser irradiation spot occurs in several molecular complexes at ambient conditions [16, 17], while some fullerene complexes, which are insensitive to laser irradiation at ambient conditions, demonstrate typical features of photopolymerization at elevated pressure [4, 5, 18]. In addition, the softening of the $A_g(2)$ mode occurs also in negatively charged fullerene molecules due to a decrease in molecular stiffness, namely the transfer of one electron from an alkali metal to a C_{60} molecule in intercalated fullerides results in the downshifting of this mode by about 6 cm^{-1} [19]. In view of this, the conclusion that pressure-induced polymerization phenomena really take place in bulk sample should be confirmed by more direct structural evidence. Thereby, it is quite necessary that the signs of polymerization, observed in the Raman spectra of fullerene complexes at high pressure, must be verified by independent *in-situ* XRD experiments in an appropriate pressure range to confirm the pressure-induced covalent bonding in the fullerene layers of a bulk sample.

In this work, we report the results of first simultaneous XRD and Raman studies of the neutral molecular donor–acceptor complex of fullerene with ferrocene, $C_{60}{\cdot}\{Fe(C_5H_5)_2\}_2$, at pressures up to 8 GPa. In 2012, the Raman study of this complex at high pressure revealed supposedly the signs of pressure-induced charge transfer and polymerization in C_{60} layers [2]. Recent Raman studies of this and several other fullerene complexes have shown that polymerization assumed in [2] may be related to the pressure-assisted photopolymerization [4, 5, 19]. Because of this, we have carried out the XRD study of high-quality single crystals of the $C_{60}{\cdot}\{Fe(C_5H_5)_2\}_2$ complex at pressures up to 5 GPa, as well as new Raman study of this complex at pressures up to 8 GPa. Our investigation is aimed at finding the structural evidence of both polymerization in fullerene layers and charge transfer at high pressure in order to verify the Raman data argued earlier in [2]. We found that the Raman spectra at high pressure exhibit peculiarities near ~ 2 GPa and ~ 4.6 GPa associated with the splitting of several phonon modes. The splitting of totally symmetric $A_g(1)$ and $A_g(2)$ modes near 4.6 GPa is irreversible and resembles typical changes associated with the formation of fullerene linear polymeric chains. Nevertheless, the XRD data and accurate structural analysis show that the unit cell volume V_0/V is a smooth and monotonous function of pressure which fits well the Murnaghan equation of state $(V_0/V)^{B'} = \{1 + P{\cdot}(B'/B_0)\}$, where $B_0 = 8.7\ GPa$ and $B' = 10.5$ are the bulk modulus and its derivative, respectively. There are no structural changes that could indicate the pressure-induced formation of interfullerene covalent bonds in C_{60} layers in the pressure range studied. At the highest pressure of 4.6 GPa, fullerene molecules are still far apart to form intermolecular covalent bonds typical of fullerene polymers. At the same time, accurate Raman measurements at 4.6 GPa show the splitting of the $A_g(2)$ phonon mode and redistribution of split component intensities which depends on the laser power and exposure time, which is typical for pressure-assisted photopolymerization in fullerene layers. In addition, the pressure dependence of the shortest distance between ferrocene and fullerene molecules demonstrates a peculiarity near 2 GPa where the linear dependence changes its slope indicating a change in the donor–acceptor interaction. This may be a reason for C_{60} symmetry disturbance and the splitting of several degenerate H_g modes observed at this pressure. Finally, our structural data clearly show that the length of a ferrocene molecule in the $C_{60}{\cdot}\{Fe(C_5H_5)_2\}_2$ complex gradually increases from 3.29 Å at ambient pressure to 3.34 Å at 4.5 GPa, whereas its length in pristine ferrocene crystals decreases with pressure. Taking into account that the length of a ferrocene molecule with the Fe^{2+} iron charge state increases from 3.29 Å to 3.4 Å for the Fe^{3+} iron charge state [20], we think that this peculiarity indicates a partial charge transfer from the ferrocene donor to the C_{60} acceptor molecules, induced by high pressure.

Experimental

The high-quality single crystals of the donor–acceptor complex C_{60}•{$Fe(C_5H_5)_2$}$_2$ were synthesized by slow evaporation of a toluene solution containing fullerene C_{60} and ferrocene $Fe(C_5H_5)_2$ molecules. The complex is crystallized in a triclinic layered structure where close-packed fullerene layers alternate with the layers of ferrocene molecules [21]. The high-quality single crystal XRD analysis performed in this work confirmed the crystal structure above with the unit cell parameters $a = 10.060(1)$ Å, $b = 11.311(1)$ Å, $c = 18.514(1)$ Å, $\alpha = 83.63(1)^o$, $\beta = 89.82(1)^o$, $\gamma = 89.46(1)^o$, $V = 2093.6(2)$ Å^3 under ambient conditions. In the fullerene layers, each C_{60} molecule is surrounded by six neighbors with the shortest distances between the molecule centers d''=10.060 Å (two neighbors) and d'=11.015 Å (four neighbors). The XRD data at high pressure were collected in series of four pressure runs with the samples of a typical size of ~ 250 μ using a four-circle Oxford Diffraction diffractometer equipped with a two-dimensional CCD Atlas S2 and a diamond anvil cell (DAC) with Boehler-type Ia anvils.

The Raman spectra were recorded in back-scattering geometry from small pieces of a split single crystal of C_{60}•{$Fe(C_5H_5)_2$}$_2$ with a diameter of ~ 80 mμ using a micro-Raman setup comprised of an Acton SpectraPro-2500i spectrograph and a CCD Pixis2K. The 532 nm line of a single mode diode pumped laser was focused on the sample by an Olympus 50× objective in a ~ 2-μm diameter spot. The laser line was suppressed by an edge filter, while the beam intensity before DAC varied from 0.7 mW to 2 mW. The measurements at high pressure were carried out using a Mao-Bell type DAC; the 4:1 methanol/ethanol mixture or silicone oil was used as a pressure transmitting medium, and the ruby fluorescence technique was used as a pressure calibration tool [22].

Results and discussion

Figure 1 shows Raman spectra of the C_{60}•{$Fe(C_5H_5)_2$}$_2$ complex, recorded at a pressure up to 6.4 GPa, laser power of 0.7 mW, and exposure time of ~ 30 min. The spectra were recorded from the same sample site upon pressure increase in the frequency region of 250–1615 cm^{-1} and are presented after the subtraction of background. The spectral region around the strong triply degenerate T_{2g} mode of a diamond, appearing at 1332 cm^{-1} at ambient pressure [23], is excluded. The phonon bands in the experimental spectra and intensity distribution between them are similar to those obtained earlier in [2]. The Raman spectrum under ambient conditions coincides basically with that of pristine C_{60} but contains additionally several phonon modes of a ferrocene molecule with the most intensive band between them at ~ 315 cm^{-1}. A number of weak ferrocene modes do not appear in the Raman spectrum of the complex, whereas several modes of ferrocene and fullerene molecules located near the diamond T_{2g} mode are excluded. As the pressure increases, the majority of Raman peaks shift to higher energies, while the $H_g(3)$ and $H_g(4)$ fullerene modes exhibit a negative pressure shift. An important feature in the Raman spectra is the splitting of fullerene modes: $H_g(4)$ and $H_g(7)$ degenerate modes split near ~ 2 GPa, whereas the most intriguing is the splitting of non-degenerate totally symmetric $A_g(1)$ and $A_g(2)$ phonon modes at a pressure of 4.6 GPa. In addition, the degenerate $H_g(1)$ and $H_g(2)$ modes initially exhibit the signs of splitting which gradually increases with pressure. The reversible with pressure splitting of the degenerate H_g modes may be related to the symmetry reduction of a fullerene molecule due to the enhancement of the donor–acceptor interaction at high pressure. At the same time, the splitting of the $A_g(1)$ and $A_g(2)$ modes is irreversible with pressure and resembles characteristic changes in the Raman spectra of pristine C_{60} upon polymerization under HPHT treatment [14].

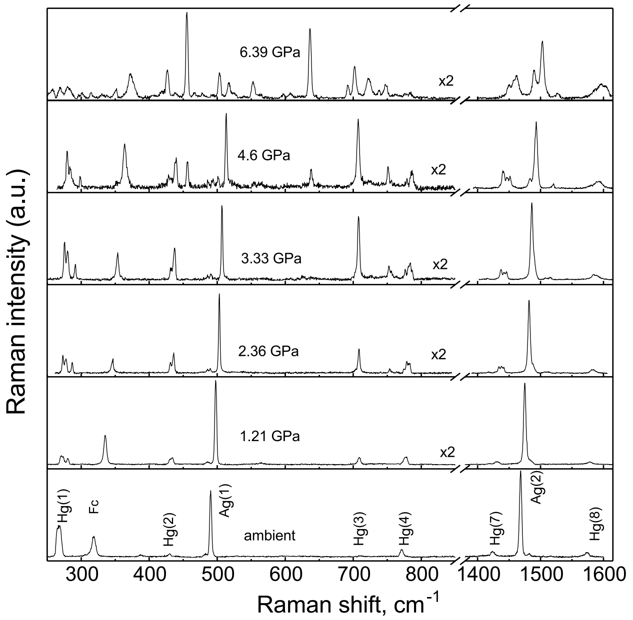

Fig. 1 Raman spectra of the C_{60}•{$Fe(C_5H_5)_2$}$_2$ complex in the energy region of 250–1615 cm^{-1} and pressure up to 6.5 GPa

Figure 2 depicts pressure dependence of the Raman modes of the C_{60}•{$Fe(C_5H_5)_2$}$_2$ complex (open circles) and two modes of pristine ferrocene and fullerene crystals (filled

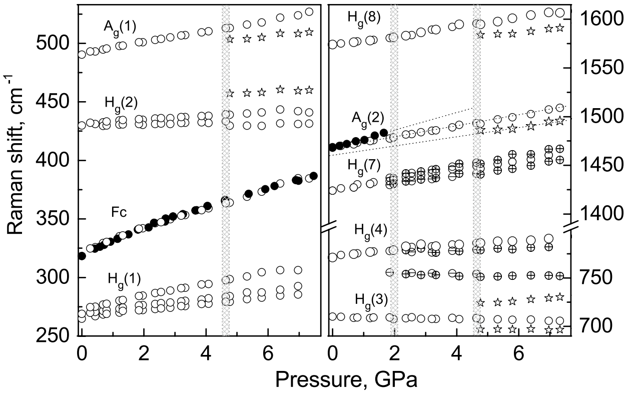

Fig. 2 Pressure dependence of the phonon modes of the C_{60}•$\{Fe(C_5H_5)_2\}_2$ complex (open circles) in the frequency regions of 250 – 533 cm^{-1} (left panel) and 690 – 1615 cm^{-1} (right panel). Filled circles – are several modes of pristine ferrocene and fullerene crystals, broken lines – are linear fits of the experimental data. Open stars and crossed circles show new modes that appeared at pressures of 2 GPa and 4.6 GPa (shaded areas)

circles); the broken lines are linear fits of some experimental data. The left and right panels illustrate the Raman data in the frequency regions of 250 – 533 cm^{-1} and 690 – 1615 cm^{-1}, respectively. The shaded areas show the pressure regions near 2 GPa and 4.6 GPa where changes in the pressure behavior of the Raman modes take place. The degenerate $H_g(4)$ and $H_g(7)$ modes split near 2 GPa, and the pressure dependence of the split components is shown with crossed circles. In addition, broad $H_g(1)$ and $H_g(2)$ modes split into two components in the initial pressure range. The splitting of all modes gradually increases with pressure and is reversible upon pressure release (not shown in the figure). Important changes occur at a pressure of 4.6 GPa when the non-degenerate $A_g(1)$ and $A_g(2)$ modes split together with the degenerate $H_g(2)$, $H_g(3)$ and $H_g(8)$ modes; the pressure dependence of newly appeared bands is shown in Fig. 2 with open stars. These changes are irreversible with pressure and resemble characteristic changes in the phonon spectrum of pristine fullerene upon HPHT and/or photo-induced polymerization [7, 10–14]. It is important to note that the linear pressure dependence of a split $A_g(2)$ mode component, extrapolated to lower pressures, provides a normal pressure frequency of ~ 1458 cm^{-1} which is characteristic of linear polymeric chains [14]. In addition, the linear pressure dependence of the $A_g(2)$ mode of pristine fullerene (filled circles) differs from that of the fullerene complex; namely, the pressure coefficient of this mode of ~ 7 cm^{-1}/GPa in pristine fullerene exceeds the corresponding value of ~ 5.5 cm^{-1}/GPa in the ferrocene complex. Note that the pressure coefficients of the $A_g(2)$ mode in a number of the donor–acceptor complexes of fullerene have nearly the same value [4, 19]. On the other hand, rather smooth pressure behavior of ferrocene phonon mode 315 cm^{-1} practically does not differ in the ferrocene complex and a pristine ferrocene crystal.

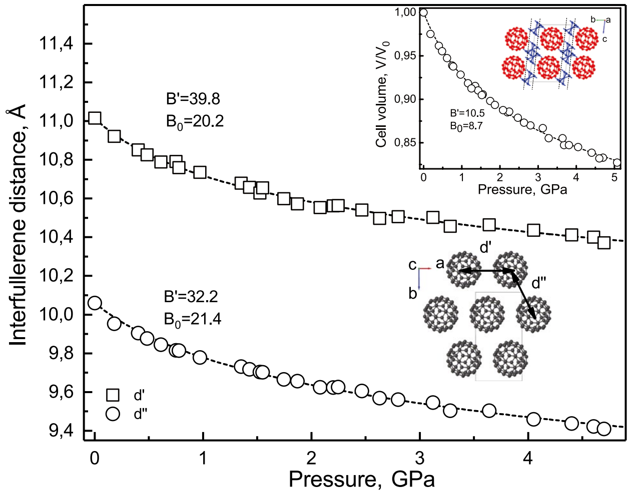

Fig. 3 Pressure dependence of the shortest distances *d'* (open squares) and *d''* (open circles) between C_{60} molecules in the C_{60}•$\{Fe(C_5H_5)_2\}_2$ complex and their fit by the Murnaghan equation of state (broken lines). Central inset: the hexagonal arrangement of the fullerene molecules along the *b* axes. Upper inset: the arrangement of the ferrocene donor and fullerene acceptor molecules along the *a* axes and pressure dependence of the cell volume V/V_0 (open circles), broken line – is fit of the experimental data by the Murnaghan equation of state

The Raman studies of the C_{60}•$\{Fe(C_5H_5)_2\}_2$ complex at high pressure in the present work and in an earlier publication [2] presumably indicate polymerization in fullerene layers near 4.6 GPa. Nevertheless, to find out that polymerization actually takes place, direct structural evidence is required. Figure 3 represents the results of a detailed structural analysis performed on the basis of single crystal XRD data obtained in this work. The upper inset in Fig. 3 depicts pressure dependence of the unit cell volume of the C_{60}•$\{Fe(C_5H_5)_2\}_2$ complex at a pressure of up to ~ 5 GPa. The pressure behavior of the relative volume V/V_0 (open circles) is fitted well by the Murnaghan equation of state (broken line):

$$\left(\frac{V}{V_0}\right)^{B'} = \{1 + P \cdot (B'/B_0)\} \tag{1}$$

Here $B_0 = 8.7$ GPa is the bulk modulus and the $B' = 10.5$ is its derivative, which are close to those of the C_{60} fullerite crystal in the simple cubic phase [24]. The pressure dependence of the cell volume is smooth and monotonous and does not show any peculiarity hinting at a phase transition. It should be taken into account that polymerization must lead to an abrupt decrease in the cell volume due to a decrease in the interfullerene distance during the formation of covalent bonds. The diagram in the inset shows arrangement of the ferrocene donor and fullerene acceptor molecules along the *a* axes, derived directly from the CIF file. The diagram in the lower right part of Fig. 3 shows hexagonal arrangement of the fullerene molecules where the *d'* and *d''* shortest distances are depicted along the *c* axes, also derived from the CIF file. The pressure dependence of the shortest distances *d'* (open squares) and *d''* (open circles) between C_{60} molecules is fitted well by a two-dimensional analog of the Murnaghan equation of state (broken lines). The pressure dependence of *d'* and *d''* is smooth and does not show any peculiarity. These data clearly indicate that fullerene molecules cannot form interfullerene covalent bonds in the pressure range under study. Indeed, the shortest distance between the centers of C_{60} molecules in the polymeric phases is close to 9.06 Å [25], whereas the shortest distance *d''* between C_{60} cages in the $C_{60}\cdot\{Fe(C_5H_5)_2\}_2$ complex at a pressure of 5 GPa is 9.4 Å. Thus, the detailed structural analysis unambiguously shows that fullerene molecules are too far apart to form interfullerene covalent bonds. With a further increase in the pressure, the distance *d''* will gradually decrease, and numerical estimates based on two-dimensional compressibility data ($B' = 32.2$ GPa and $B_0 = 21.4$, see Fig. 3) and two-dimensional analog of Murnaghan equation of state $(d''/d''_o)^{-B'} = \{1 + P\cdot(B'/B_0)\}$ provide a value of 9.06 Å at P = 18.5 GPa if no phase transitions occur at intermediate pressures.

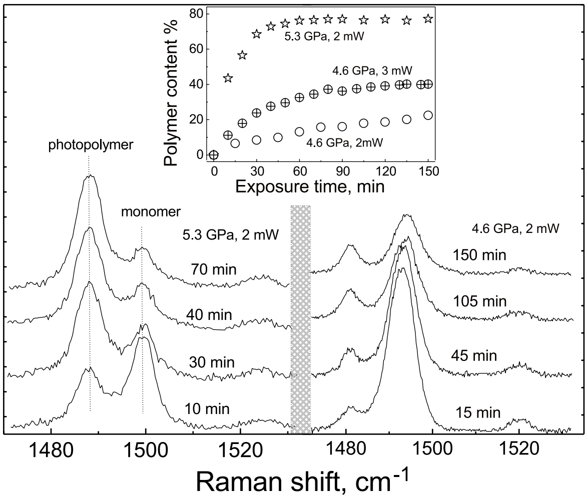

Fig. 4 Time evolution of the Raman spectra of the $C_{60}\cdot\{Fe(C_5H_5)_2\}_2$ complex in the region of the $A_g(2)$ mode under pressures 4.6 GPa and 5.3 GPa, laser power of 2 mW. Inset: polymer content as a function of the laser exposure time under various pressure and laser power conditions

The structural data at high pressure show that the previously reported Raman observation of polymerization at pressures between 4 and 5 GPa [2] does not take place. We strongly believe that changes in the Raman spectra in this pressure range are due to photopolymerization upon laser irradiation. Moreover, the manifestation of pressure-assisted photopolymerization was clearly shown in a recent Raman study of this complex [5]. In view of this, we carefully examined the transformations of the Raman spectra upon laser irradiation at various pressures, laser powers, and exposure times. Figure 4 shows time-dependent changes in the Raman spectra of the $C_{60}\cdot\{Fe(C_5H_5)_2\}_2$ complex in the region of the $A_g(2)$ mode. The right spectra refer to a pressure of 4.6 GPa and laser power of 2 mW. The Raman spectra show the splitting of the $A_g(2)$ mode and a gradual increase in the split component intensity with an increasing laser exposure time. The total intensity of the split $A_g(2)$ mode component, associated with fullerene linear polymeric chains, with respect to the total intensity of two bands defines the content of the photopolymerised material. This value is depicted in the inset of Fig. 4 with open circles showing an increase in the polymer content with exposure time. The crossed circles demonstrate the dependence at a higher laser power of 3 mW when photopolymerization is intensified. The left spectra were taken at a pressure of 5.3 GPa and laser power of 2 mW. Photopolymerization under these conditions becomes considerably faster as it follows from dependence of the polymer content on the exposure time, shown in the inset with open stars. Note that in all three series of Raman measurements the spectra were taken from a fresh place of the sample. Photopolymerization does not occur at pressures lower than 4.6 GPa under similar conditions of laser power and exposure time as it follows from Fig. 1. Thus, high pressure is necessary to initiate photopolymerization, but the reason why this happens is not entirely clear. The polymerization via the 2 + 2 cyclo-addition reaction requires the parallel orientation of double C = C bonds of neighboring C_{60} molecules. In a pristine fullerene crystal, the double C = C bond of molecules is directed to the center of the pentagon (P-orientation) or hexagon (H-orientation) of an adjacent molecule. The parallel orientation of double C = C bonds can be reached upon hopping of molecules between the P- and H-orientations, known as rotations of C_{60} cages. Therefore, both laser irradiation and rotation of molecules are necessary for photopolymerization. The calculated energy barrier between the P and H orientations in pristine C_{60} is about ~ 0.3 eV, while the experimentally determined activation energy of molecular rotations is ~ 0.24 eV; this magnitude allows molecular rotations under ambient conditions [26, 27]. The energy barrier in the $Pt(dbdtc)_2\}\bullet C_{60}$ and $\{Pt(nPr_2dtc)_2\}\bullet(C_{60})_2$ fullerene molecular complexes is even smaller most likely due to the influence of donor molecules because of the donor–acceptor interaction [27]. In several molecular complexes with an initially large energy barrier between the P- and H-orientations, the rotations of molecules and hence photopolymerization under ambient conditions are inhibited, but they can appear at an elevated pressure [4, 5, 19]. In our opinion, an increase in the donor–acceptor interaction at high pressure may lead to a decrease in the barrier magnitude which activates molecular rotations and promotes photopolymerization.

The peculiarities of intermolecular interaction between ferrocene donor and fullerene acceptor molecules at high pressure are shown in Fig. 5. The left panel depicts experimental pressure dependence of the shortest distance between a fullerene molecule and the nearest cyclopentadienyl ring of a ferrocene molecule (open circles); the broken line is a linear fit of the experimental data. The dependence shows a peculiarity near ~ 2 GPa where the slope of linear fit changes abruptly indicating the change in intermolecular interaction. This anisotropic interaction is concentrated on one side of a fullerene molecule that can result in symmetry disturbance. Indeed, the splitting of some H_g modes of the fullerene molecule in the Raman spectra at 2 GPa may be associated with the enhancement of anisotropic donor–acceptor interaction. Surprisingly, our data show that the ferrocene molecule length gradually increases with pressure, while one would expect the reverse pressure behavior (Fig. 5, central panel). Namely, the length of a ferrocene molecule in the complex gradually increases with pressure (open squares). The broken line is linear fit of the experimental data 3.3 Å + P•0.009 Å/GPa. Thus, the initial length of a ferrocene molecule of 3.291 Å at ambient pressure increases to 3.344 Å at 4.5 GPa. To understand better this unusual behavior we performed the XRD study of a pristine ferrocene single crystal at high pressure. As expected, the length of a ferrocene molecule in the case of a ferrocene single crystal decreases with pressure (open circles). The broken line is a linear fit of the experimental data 3.3 Å-P•0.006 Å/GPa. We suppose that an increase in the ferrocene molecule length in the fullerene complex is due to a pressure-induced charge transfer from the ferrocene donor to the C_{60} acceptor molecules. Really, the published structural data specify a change in the ferrocene molecule length depending on the iron valence state. The right panel in Fig. 5 depicts systematized data from the Cambridge Structural Database (CCDC) [20] related to the dependence of the ferrocene molecule length on the valence state of an iron atom. The data are presented in the form of a histogram which shows the number of communications vs. the reported length of the ferrocene molecule with two different valences of the iron atom. According to these data, the length of the ferrocene molecule under ambient conditions increases from ~ 3.29 Å for Fe^{2+} to ~ 3.40 Å for Fe^{3+}. In light of this, the data shown above mean that the valence of the iron atom in the ferrocene donor molecule gradually increases from 2^+ to 3^+ when the pressure increases. In other words, the application of high pressure to the C_{60}•$\{Fe(C_5H_5)_2\}_2$ complex stimulates the charge transfer from the ferrocene donor to the fullerene acceptor molecule. Thus, at a pressure of ~ 4.5 GPa the partial charge transfer results in the intermediate oxidation state of the iron atom, whereas the complete transfer of one electron may be expected at a pressure of ~ 8 GPa. The observed charge transfer may be due to the high-pressure stimulated overlap of the electron orbitals of the donor and acceptor molecules and changes in their electron energy spectra. Note that some indirect indications of the charge transfer can be found in the pressure behavior of the $A_g(2)$ fullerene mode that demonstrates smaller pressure shift coefficients in the donor–acceptor complexes as compared with pristine fullerite crystals. The values of initial interfullerene distances and bulk modulus of a pristine fullerene crystal and fullerene complexes differ quite slightly, so the difference in pressure shift coefficients may be related to a gradual charge transfer and the softening of these modes with pressure. The effect of simultaneous positive pressure-induced shift and softening of the mode due to charge transfer leads to a decrease in the total pressure shift coefficient.

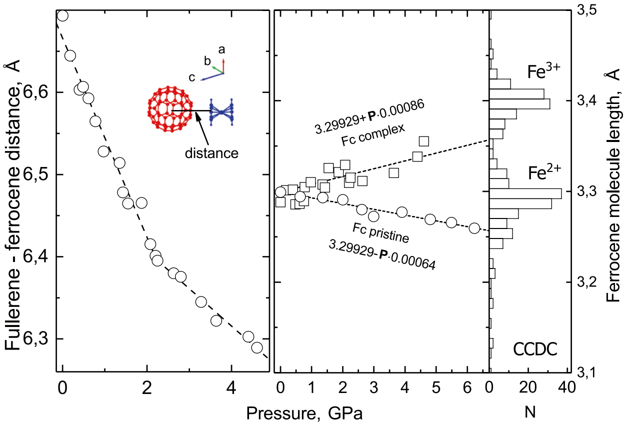

Fig. 5 Left panel: pressure dependence of the shortest distance between the ferrocene and fullerene molecules (open circles), broken line is linear fit of the experimental data. Central panel: pressure dependence of the ferrocene molecule length in the complex (open squares) and in a pristine crystal (open circles), broken lines are linear fits of the experimental data. Right panel: histogram of the systematized data on the ferrocene molecule length depending on the oxidation state of an iron atom (CCDC database)

Conclusions

Summarizing, the Raman spectra of the C_{60}•$\{Fe(C_5H_5)_2\}_2$ complex at high pressure manifest peculiarities near ~ 2 GPa and ~ 4.6 GPa associated with the splitting of various phonon modes. The splitting of totally symmetric $A_g(1)$ and $A_g(2)$ modes near 4.6 GPa resembles that typical of the formation of fullerene polymeric chains. The XRD study of the high-quality single crystals at a pressure of up to 5 GPa shows smooth and monotonous pressure dependence of the unit cell volume V/V_0 that fits well to the Murnaghan equation of state $(V_0/V)^{B'} = \{1 + P\cdot(B'/B_0)\}$ with

$B_0 = 8.7$ GPa and $B' = 10.5$. There are no observed structural changes that could indicate the pressure-induced formation of interfullerene covalent bonds in C_{60} layers in the pressure range studied. At a pressure of 4.6 GPa, the shortest distance between fullerene molecules is 9.4 Å that is far enough from the intermolecular distances characteristic of fullerene polymers. The numerical estimates based on compressibility data provide an intermolecular distance of 9.06 Å, typical for fullerene polymers, at $P \geq 18.5$ GPa if no phase transitions occur at intermediate pressures. It has been revealed that changes in the Raman spectra at pressures higher than 4.6 GPa are related to pressure-assisted photopolymerization in fullerene layers which intensifies at an increased laser power and pressure. Photopolymerization at high pressure may be associated with the appearance of fullerene molecule rotations. This may be due to a pressure-induced decrease in the initially high energy barrier between the H and P fullerene orientations that inhibits molecular rotations under ambient conditions. The pressure dependence of the distance between the ferrocene and fullerene molecules shows a peculiarity near 2 GPa. This is associated with the enhancement of the anisotropic donor–acceptor interaction at high pressure which leads to the disturbance of fullerene molecule symmetry resulting in the splitting of several Raman modes. Finally, the structural data show that the length of the ferrocene molecule in the complex gradually increases with pressure from ~ 3.29 Å for the Fe^{2+} charge state to ~ 3.40 Å for the Fe^{3+} charge state. Definitely, high pressure stimulates the charge transfer from the ferrocene donor to the fullerene acceptor molecule in the $C_{60}{\cdot}\{Fe(C_5H_5)_2\}_2$ complex.

Acknowledgments This work is carried out within the state task of ISSP.

References

1. Meletov KP, Dolganov VK, Spitsina NG, Yagubskii EB, Arvanitidis J, Papagelis K, Ves S, Kourouklis GA (1997) Pressure-Induced Charge-Transfer Phase Transition in Crystalline $C_{60}{*}C_{10}H_{12}Se_4{*}2(CS_2)$ Molecular Complex Studied by Raman Spectroscopy. Chem Phys Lett 281:360–365
2. Cui W, Yao M, Liu D, Li Q, Liu R, Zou B, Cui T, Liu B (2012) Reversible polymerization in doped fullerides under pressure: the case of C60•{Fe(C5H5)2}2. J Phys Chem B 116:2643–2650
3. Meletov KP, Konarev DV (2012) Raman study of the pressure-induced phase transitions in the molecular donor-acceptor complex $\{Pt(dbdtc)_2\}{\bullet}C_{60}$. Chem Phys Lett 553:21–25
4. Meletov KP, Konarev DV, Tolstikova AO (2015) Phase transitions and photoinduced transformations at high pressure in the molecular donor-acceptor fullerene complex $\{Cd(dedtc)_2\}_2{\bullet}C_{60}$. JETP 120:989–997
5. Kato K, Murata H, Gonnokami H, Tacibana M (2016) Polymerization in ferrocene-doped C_{60} nanosheets under high pressure and light irradiation. Carbon 107:622–627
6. Sun S, Gui W, Shuangming W, Liu B (2017) Investigation of the polymerization mechanism of ferrocene doped C_{60} under high pressre and high temperatre. Sci Rep 7:10809-1-10809–6
7. Rao AM, Zhou P, Wang KA, Hager GT, Holden JM, Wang Y, Lee WT, Bi XX, Eklund PC, Cornett DS, Duncan MA, Amster IJ (1993) Photoinduced polymerization of solid C_{60} films. Science 259:955–957
8. Pusztai T, Oszlanyi G, Faigel G, Kamaras K, Granasy L, Pekker S (1999) Bulk structure of phototransformed C_{60}. Solid State Commun 111:595–599
9. Karachevtsev VA, Mateichenko PV, Nedbailo NY, Peschanskii AV, Plokhotnichenko AM, Vovk OM, Zubarev EN, Rao AM (2004) Effective photopolymerization of C_{60} films under simultaneous deposition and UV light irradiation: Spectroscopy and morphology study. Carbon 42:2091–2098
10. Iwasa Y, Arima T, Fleming RM, Siegrist T, Zhou O, Haddon RC, Rothberg LJ, Lyons KB, Karter HL Jr, Hebard AF, Tycko R, Dabbagh G, Krajewski JJ, Thomas GA, Yagi T (1994) New phases of C_{60} synthesized at high pressure. Science 264:1570–1572
11. Nunez-Regueiro M, Marques L, Hodeau JL, Bethoux O, Perroux M (1995) Polymerized fullerite structures. Phys Rev Lett 74:278–281
12. Rao AM, Ecklund PC, Hodeau J-L, Marques L, Nunez-Regueiro M (1997) Infrared and Raman studies of pressure-polymerized C_{60}. Phys Rev B 55:4766–4773
13. Zhou P, Dong ZH, Rao AM, Ecklund PC (1993) Reaction mechanism for photopolymerization of solid fullerene C_{60}. Chem Phys Lett 211:337–340
14. Senyavin VM, Davydov VA, Kashevarova LS, Rakhmanina AV, Agafonov V, Allouchi H, Ceolin R, Sagon G, Szwarc H (1999) Spectroscopic properties of individual pressure-polymerized phases of C_{60}. Chem Phys Lett 313:421–425
15. Davydov VA, Kashevarova LS, Rakhmanina AV, Senyavin VM, Ceolin R, Szwarc H, Allouchi H, Agafonov V (2000) Spectroscopic study of pressure polymerized phases of C_{60}. Phys Rev B 61:11936–11945
16. Meletov KP, Velkos G, Arvanitidis J, Christofilos D, Kourouklis GA (2017) Raman study of the photopolymer formation in the $\{Pt(dbdtc)_2\}{\cdot}C_{60}$ fullerene complex and the decomposition kinetics of the photo-oligomers. Chem Phys Lett 681:124–129
17. Meletov KP (2018) Photopolymerization in the fullerene layers of the molecular donor-acceptor complex $\{Pt(nPr_2dtc)_2\}{\cdot}(C_{60})_2$. Phys Solid State 60:2103–2108
18. Kuzmin AV, Konarev DV, Khasanov SS, Meletov KP (2018) Crystal structure and Raman spectra of molecular complex $[Cd(Et_2dtc)\}_2{\cdot}DABCO]{\cdot}C_{60}{\cdot}(DABCO)_2$ at high pressure. Nanosystems: Physics, Chemistry, Mathematics 9(1):23–37
19. Winter J, Kuzmany H, Soldatov A, Persson P-A, Jacobson P, Sundqvist B (1996) Charge transfer in alkali-metal-doped polymeric fullerenes. Phys Rev B 54:17486–17492
20. Groom CR, Bruno IJ, Lightfoot MP, Ward SC (2016) The Cambridge Structural Database. Acta Cryst B 72:171–179
21. Crane JD, Hitchcock PB, Kroto HW, Taylor R, Walton DRM (1992) Preparation and characterisation of C_{60}(ferrocene)$_2$. J Chem Soc Chem Commun Royal Society of Chemistry 24:1764–1765
22. Jayaraman A (1986) Ultrahigh pressures. Rev Sci Instrum 57:1013–1031
23. Solin SA, Ramdas AK (1970) Phys Rev B 1:1687–1698

24. Lundin A, Sundqvist B (1996) Compressibility of C_{60} in the temperature range 150–335 K up to a pressure of 1 GPa. Phys Rev B 53:8329–8336
25. Narymbetov B, Agafonov V, Davydov VA, Kashevarova LS, Rakhmanina AV, Dzyabchenko AV, Kulakov VI, Ceolin R (2003) The crystal structure of the 2D polymerized tetragonal phase of C_{60}. Chem Phys Lett 367:157–162
26. Burgos E, Halac E, Bonadeo H (1994) Intermolecular forces and phase transitions in solid C_{60}. Phys Rev B 49:15544–15549
27. Meletov KP (2020) The photopolymerization rate and activation energy of C_{60} rotations in fullerene and its molecular complexes. Fullerenes, Nanotubes, Carbon Nanostruct 28(2):93–96